Skeletal Radiol (2000) 29:439–446

ARTICLE

André Stürzenbecher
Jürgen Braun
Stefan Paris
Thomas Biedermann
Bernd Hamm
Matthias Bollow

MR imaging of septic sacroiliitis

Received: 1 November 1999
Revision requested: 4 January 2000
Revision received: 14 April 2000
Accepted: 16 May 2000

A. Stürzenbecher, M.D. · B. Hamm, M.D.
M. Bollow, M.D. (✉)
Humboldt-Universität zu Berlin,
Department of Radiology,
Charité Medical School,
Schumannstrasse 20/21,
10117 Berlin, Germany

J. Braun, M.D.
Freie Universität Berlin,
Benjamin Franklin Medical School,
Department of Nephrology
and Rheumatology,
Hindenburgdamm 30,
12200 Berlin, Germany

S. Paris, M.D.
Unfallkrankenhaus Berlin,
Department of Radiology,
Brebacher Weg 15,
12683 Berlin, Germany

T. Biedermann, M.D.
Krankenhaus Berlin-Buch,
II. Kinderklinik, Wittbergstrasse 50,
13125 Berlin, Germany

Abstract *Objective*. To investigate the diagnostic value of magnetic resonance (MR) imaging in detecting septic sacroiliitis and to determine whether the MR characteristics allow this entity to be differentiated from sacroiliitis in spondylarthropathy (SpA).
Patients and design. The imaging findings of 11 patients with septic sacroiliitis were retrospectively analyzed by two experienced radiologists. Radiographic surveys of the pelvis as well as computed tomography (CT) and MR images of the sacroiliac joints were available in all cases. Seven of the patients additionally underwent a follow-up MR examination. The MR imaging protocol comprised combinations of coronal and transverse T1-weighted spin-echo (SE) or fast SE sequences, T2-weighted gradient-echo (GE) sequences and short tau inversion recovery sequence (STIR) sequences as well as dynamic contrast-enhanced T1-weighted acquisitions.
Results. Three patients with a short disease history showed anterior and/or posterior subperiosteal infiltrations ("lava cleft phenomenon"), transcapsular infiltrations of juxtaarticular muscle layers, which obscured the fasciae, and periarticular bone marrow edema. The eight patients with more advanced stages of sacroiliitis additionally showed abscess formation, sequestration, and erosion. At follow-up MR examination (n=7) under systemic antibiotic treatment, the morphologic characteristics showed progression (n=1), regression (n=4), unchanged findings (n=1), or a mixed response (n=1). Clinical improvement precedes resolution of the MR findings.
Conclusions. Anterior and/or posterior subperiosteal infiltrations and transcapsular infiltrations of juxtaarticular muscle layers were depicted in all patients. These MR imaging findings are characteristic of septic sacroiliitis and may be used to differentiate this entity from sacroiliitis in SpA.

Key words Magnetic resonance (MR) imaging · Sacroiliac joint · Septic sacroiliitis

Introduction

Septic sacroiliitis is a uncommon [1, 2, 3, 4, 5] although its incidence has increased in recent years, and accounts for about 1.5% of all cases of pyogenic arthritis in pediatric patients and for less than 1% in adults [5, 6, 7]. The disease occurs secondary to primary infections of the skin and mucosa [2, 7, 8, 9], the skeleton, and the urogenital tract [10] or after trauma [2, 6, 11, 12]. Other predisposing factors are pregnancy [10, 13], endocarditis [3], drug and alcohol addiction [3, 10, 14, 15, 16], and malignant disease [8]. The pathogens typically reach the sacroiliac joint (SIJ) by hematogenous spread, and less commonly by local extension from infection of adjacent

Table 1 Infectious agents

Acute form [14, 20, 21]	Chronic form [1, 3, 5, 7, 19]
Staphylococcus aureus	*Streptococcus* species
Streptococcus species	*Pneumococcus* species
Enterococcus species	*Pseudomonas aeruginosa*
	Serratia species
	Escherichia coli

soft tissue or bone [5]. Furthermore, pregnancy and delivery may lead to loosening of the SIJs, thereby possibly inducing local inflammatory changes [1, 5, 12, 17]. SIJ infection is nearly always a unilateral process [5, 18].

Staphylococcus aureus is the most frequent pathogen isolated in all age groups but other common infectious agents are listed in Table 1. The chronic form is observed in about 10% of patients with skeletal tuberculosis [3, 19, 22, 23] or systemic brucellosis [19, 24]. Between 25% and 67% of patients are reported to have a positive blood culture [18, 25], but in about 40% of cases the primary site of infection is not identified [12, 18].

Besides an elevated blood sedimentation rate, leukocytosis, and elevated temperatures, septic sacroiliitis typically presents with nonspecific clinical symptoms [5, 6, 26] and may thus mimic other disease entities such as disk protrusion [8, 13, 26, 27], septic hip [8, 11, 13, 27] or appendicitis [2, 6, 21, 28]. The anatomic position of the SIJs severely limits assessment by physical examination [29].

The full range of imaging modalities have traditionally been employed in these patients and magnetic resonance (MR) imaging has been increasingly used to diagnose septic sacroiliitis [10, 16, 30].

Before the use of antibiotics, mortality in children was 30–40% [27, 31]. Today septic sacroiliitis presents a diagnostic rather than a therapeutic problem since the timely administration of antibiotics will lead to restitution without surgical intervention [2, 5, 6, 8, 12].

The difficulties in early clinical diagnosis delay the initiation of treatment [5, 12, 16, 18], and therefore imaging modalities have a major role in diagnosis [5, 29].

This retrospective analysis was undertaken to assess the MR features of septic sacroiliitis that would confirm the diagnosis at an early stage and to determine whether they differ from the reported MR appearance of sacroiliitis in spondylarthropathy (SpA).

Materials and methods

Patients

A retrospective analysis was performed in 11 patients (9 female, 2 male; mean age 25 years, range 10–58 years) examined between 1994 and 1999 with the diagnosis of unilateral septic sacroiliitis (8 right, 3 left) confirmed by CT-guided biopsy, surgery, and/or blood culture (by microbiology and/or histology).

All patients underwent anteroposterior pelvis radiography, postcontrast CT scanning, and MR imaging of the SIJ. Seven of the patients were additionally followed up by MR imaging.

MR imaging

The initial enhanced MR examination was performed in the 11 patients within 2–122 days of the first manifestation of clinical symptoms. Follow-up by MR imaging in seven of the patients was performed 6 days to 25 weeks after the initial MR examination.

The patients were examined in the supine position with mild flexion of the hip and knee joints, on a 1.5-T MR system (Magnetom Vision, Siemens, Erlangen, Germany) with a phased-array coil using the following sequences: coronal and transverse T1-weighted spin-echo (SE) (TR/TE: 500/15 ms) or fast SE sequences (TR/TE: 500/10 ms), T1-weighted gradient-echo (GE: fast low angle shot) sequence (TR/TE: 50/7 ms; flip angle 70°), T2-weighted GE sequences (TR/TE: 325/12 ms; flip angle 30°), and a short tau inversion recovery sequence (STIR) (TR/TI/TE: 4000/150/60 ms). In all cases the dynamic MR examination was performed using the same T1-weighted sequence. The procedure takes 8 min, with a delay of 1 s between the eight repeated measurements (53 s each). After the first measurement, the contrast agent gadolinium diethylene triaminepentaacetic acid (Gd-DTPA; Magnevist, Schering, Berlin, Germany) was administered as one bolus in a concentration of 0.1 mmol/kg body weight. The follow-up MR examinations were carried out with identical adjustments.

Analysis

Radiographs and MR images of the 11 patients were evaluated by two senior radiologists (M.B., S.P.) independently in a different, randomized order to allow individual assessment for radiographic examinations and for each of the 22 MR imaging studies. Differences were resolved by discussion.

Plain radiographic features evaluated included blurring/erosions of joint margins and widening of the joint space and were rated as absent (0), probable (+), likely present (++), and definitively present (+++). On the MR images, the readers had to identify and grade the following pathomorphologic patterns: anterior and/or posterior subperiosteal infiltration; bone marrow edema; muscle infiltration including iliopsoas, erector spinae and the glutei; abscess formation; sequestra; and erosions.

Inflammation of the SIJ was characterized by a reduced signal intensity (SI) of the joint space on T1-weighted images and an increased SI on STIR and T2-weighted sequences. Anterior and/or posterior subperiosteal infiltration, periarticular bone marrow edema, and transcapsular infiltration of soft tissue/muscle showed a reduced SI on T1-weighted sequences and an increased SI on STIR and T2-weighted sequences. The inflammatory changes showed pronounced Gd-DTPA enhancement on the postcontrast images.

The MR appearance of abscess is hypointense on T1-weighted images and hyperintense on STIR and T2-weighted images. Postcontrast images show a pronounced peripheral enhancement and a nonenhancing center. Sequestra were depicted by all sequences as signal-free intra-articular fragments without contrast enhancement. Erosions were seen as areas of contrast enhancement showing hypointensity on the T1-weighted images and hyperintensity on the T2-weighted/STIR images before Gd-DTPA administration. They disrupt the continuity of the juxta-articular cortical substance.

The scale used for grading the MR images was the same as that used for assessing the radiographs. Two readings of the MR images were performed: the first without the contrast-enhanced sequences, the second including the contrast-enhanced sequences.

Results

Data regarding age, sex, interval between onset of symptoms and preliminary diagnosis, confirmation of the infectious agent, cause, and type of treatment are summarized in Table 2. Three patients (cases 4, 6 and 9) who underwent primary surgical management were examined by MR imaging only once. Seven cases were followed up by MR imaging (Table 3; Fig. 1). In case 1, in which there was complete clinical resolution, recurrence was diagnosed 140 days later.

Anterior and/or posterior subperiosteal infiltration, periarticular bone marrow edema as well as transcapsular infiltrations of the juxta-articular anterior and/or posterior muscle groups obscuring of the fasciae were visualized in all infected SIJs with varying degrees of severity (Figs. 1, 2, 3, 4; Table 3). Anterior primary muscle infiltration occurred in nine cases while two cases (cases 5, 11) involved the posterior muscle group. In all cases infiltration was accompanied by displacement of the fatty lamella of the adjacent muscles (Fig. 1C).

Abscess formation (Fig. 3), sequestration, and erosion (Fig. 4A) were the initial findings in the eight cases with advanced disease (Table 3). In a patient with early sacroiliitis (case 1), an abscess was identified only at follow-up, suggesting progression of the disease.

Table 2 Clinical information and bacteriology (*CT-B* CT-guided biopsy, *BC* blood culture, *UC* urinary culture, *NA* not available, *AT* antibiotic therapy, *ST* surgical treatment)

Case no.	Gender	Age (years)	Culture	Organism	Underlying disease/ predisposing conditions	Therapy
1	F	12	BC	*Staphylococcus aureus*	Trauma	AT
2	F	39	BC, CT-B	*Staphylococcus aureus*	Unknown autoimmune deficiency	AT
3	M	10	BC, UC	*Enterococcus faecalis*	Urinary tract infection	AT
4	M	58	CT-B	*Staphylococcus aureus*	Deep felon	ST
5	F	41	CT-B	Beta-haemolys. *Streptococcus*	Suppurative tonsillitis	AT/ST
6	F	25	CT-B	*Staphylococcus aureus*	Drug abuse	ST
7	F	28	CT-B	*Streptococcus agalactinae*	Post-partum	AT
8	F	11	BC	NA	NA	AT
9	F	27	CT-B	*Staphylococcus aureus*	Dug abuse	AT/ST
10	F	11	BC	NA	Suppurative tonsillitis	AT
11	F	11	BC	NA	NA	AT

Table 3 Radiographic and MR imaging findings [(0) normal, (+) suspicious, (++) minimally abnormal, (+++) definitively abnormal]

Case no.	Interval (days)[a]	Conventional radiography	Subperiosteal infiltration	Bone marrow edema	Muscle infiltration		Abscess	Sequestration	Erosion
					Anterior[b]	Posterior[c]			
1	2	0	+++	+	+++	0	0	0	0
1	8		+++	+++	+++	++	+++	0	0
1	150	+++	+++	+++	+++	++	++	+	++
2	120	++	+++	+++	+++	0	+++	+++	+++
2	300		+++	+++	+++	0	+++	+++	+++
3	14	0	+++	+++	+++	0	0	0	0
3	74		0	0	0	0	0	0	0
4	90	++	+++	+++	+++	+++	+++	+++	+++
5	60	++	+++	+++	0	++	+++	+	+++
5	107		+++	++	0	+	++	++	+++
6	90	+++	++	+++	+	+	+++	++	+++
7	35	+++	+++	+++	+++	+++	+++	+++	+++
7	50		+++	+++	++	+++	+++	+++	+++
7	74		+++	+++	++	+	0	+++	+++
8	10	0	+++	+++	++	0	0	0	0
8	31		+	+	0	0	0	0	0
8	70		0	0	0	0	0	0	0
9	90	+++	+++	+++	+++	++	+++	+++	+++
10	122	+	++	+++	+++	+	++	0	+
11	30	+	+++	+++	+	+++	0	0	+++
11	116		+++	+++	+	+++	0	0	+++
11	145		+++	+++	+	+	0	0	+++

[a] Interval between onset of symptoms and preliminary diagnosis
[b] Anterior: iliopsoas muscle
[c] Posterior: greatest and middle gluteal muscles, erector muscle

Three patients (cases 1, 3, 8) with a short disease history (delay until diagnosis: mean 13 days, range 2–14 days) showed anterior and/or posterior subperiosteal infiltration, periarticular bone marrow edema as well as infiltration of pericapsular muscle layers. These changes were interpreted as early inflammatory signs of septic sacroiliitis.

All patients underwent systemic antibiotic treatment. Follow-up of treatment by MR imaging demonstrated progression of the MR features in only one patient (case 1), in whom a newly formed abscess was identified after 6 days. Four patients (cases 3, 7, 8, 11) showed regression (Fig. 1), and one patient (case 2) had unchanged findings. Case 5 showed a mixed response with resolution of the abscess but progressive sequestration. In cases 7 and 11, the MR features were seen to persist for a long time despite early clinical resolution, and clear-cut regression on MR imaging was seen only after a prolonged course of antibiotic (Table 3).

The two readings of the MR images – without and with inclusion of the contrast-enhanced images – clearly demonstrated the gain in diagnostic confidence achieved

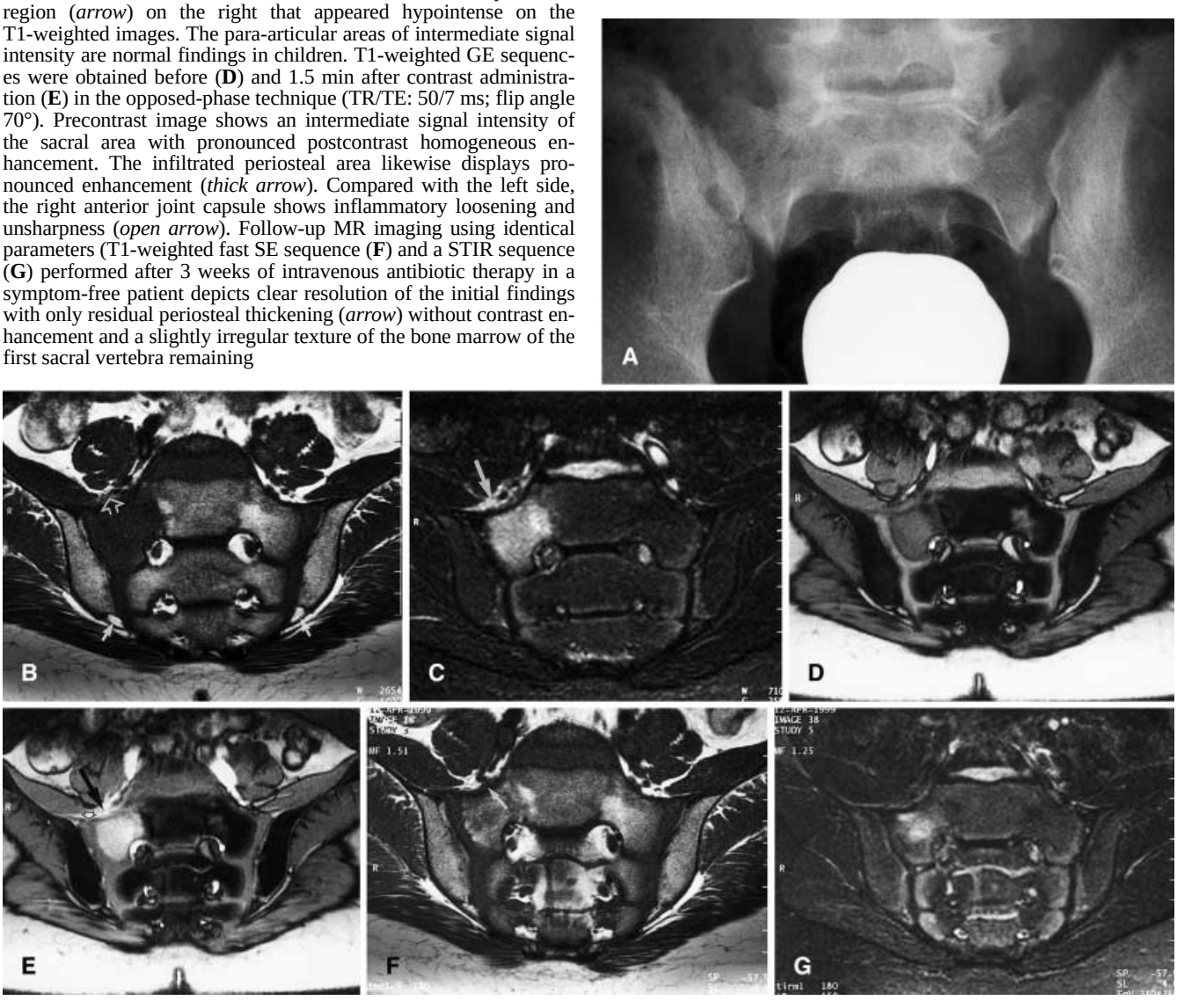

Fig. 1A–G Case 8. Images of a 10-year-old girl presenting with a 10-day history of right-sided back pain and febrile temperatures of 40 °C. A radiographic survey of the pelvis and sacroiliac joints (**A**) revealed no pathologic findings. An MR examination was performed on the next day (**B–E**). Paraxial T1-weighted fast SE sequence (**B**) (TR/TE: 500/10 ms) shows reduced signal intensity of the right ala of the first sacral vertebra masking the joint, with anterior infiltration of the intermuscular parapelvic fatty tissue (*open arrow*) obscuring the muscular fascia and periosteal swelling of the sacrum. The posterior ligamentous compartment of the capsule and the paraglenoid sulcus display the normal signal intensity of fat bilaterally (*filled arrows*). The STIR sequence in the identical orientation (**C**) (TR/TI/TE: 4000/150/60 ms) shows hyperintensity of those areas of the sacral bone marrow and of the anterior subperiosteal region (*arrow*) on the right that appeared hypointense on the T1-weighted images. The para-articular areas of intermediate signal intensity are normal findings in children. T1-weighted GE sequences were obtained before (**D**) and 1.5 min after contrast administration (**E**) in the opposed-phase technique (TR/TE: 50/7 ms; flip angle 70°). Precontrast image shows an intermediate signal intensity of the sacral area with pronounced postcontrast homogeneous enhancement. The infiltrated periosteal area likewise displays pronounced enhancement (*thick arrow*). Compared with the left side, the right anterior joint capsule shows inflammatory loosening and unsharpness (*open arrow*). Follow-up MR imaging using identical parameters (T1-weighted fast SE sequence (**F**) and a STIR sequence (**G**) performed after 3 weeks of intravenous antibiotic therapy in a symptom-free patient depicts clear resolution of the initial findings with only residual periosteal thickening (*arrow*) without contrast enhancement and a slightly irregular texture of the bone marrow of the first sacral vertebra remaining

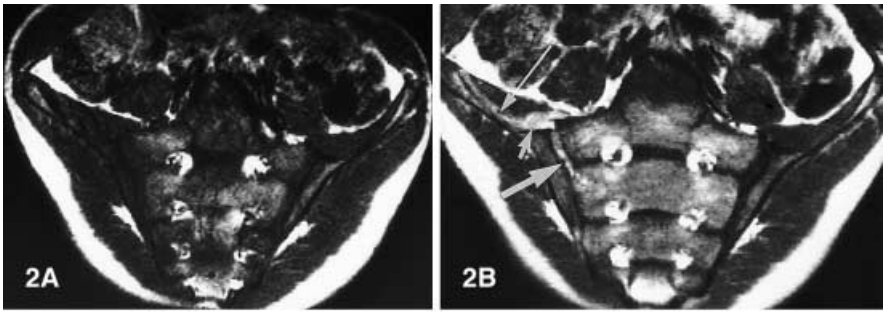

Fig. 2A, B Case 3. Paraxial T1-weighted precontrast (**A**) and postcontrast (**B**) images (SE; TR/TE: 500/15 ms) of a 10-year-old patient with symptoms and febrile temperatures of up to 39.5 °C persisting for 10 days. There is enhancement of the right joint space (*large arrow*) with infiltration destroying the capsule and extending into the subperiosteal area of the ilium (*small arrow*) and sacrum and into the iliac muscle (*small long arrow*) consistent with the "lava cleft phenomenon". Microbiologic confirmation of septic sacroiliitis caused by *Enterococcus faecalis* was obtained by means of CT-guided puncture

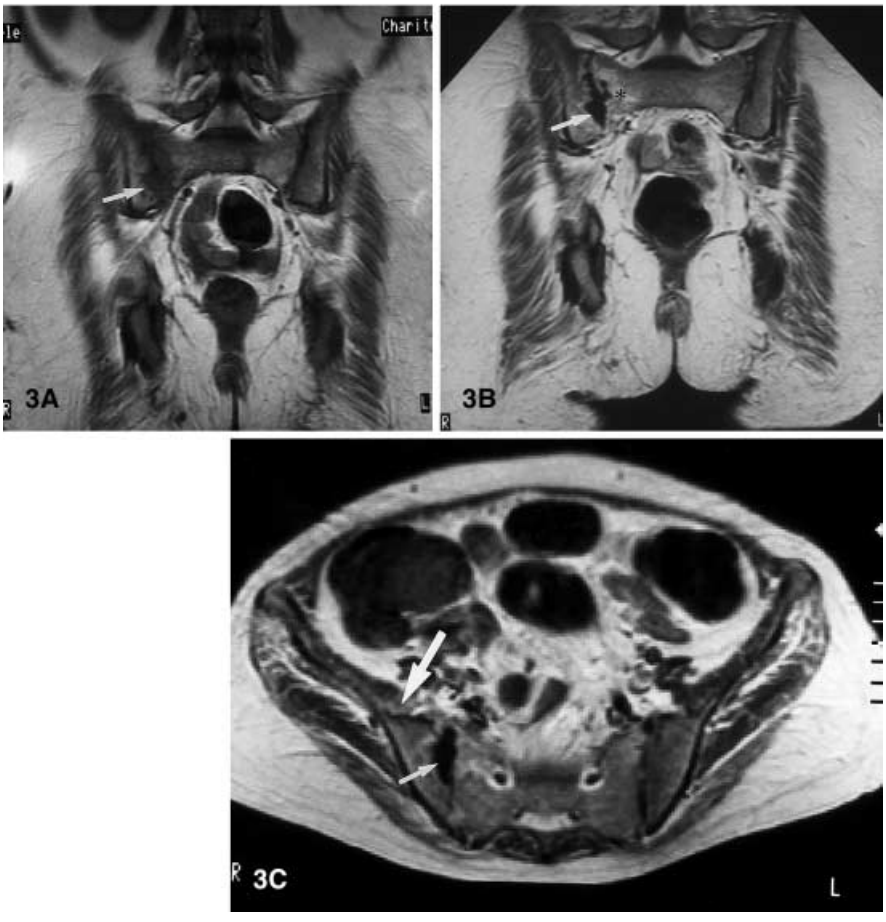

Fig. 3A–C Case 5. Coronal precontrast (**A**) and postcontrast (**B**) and axial (**C**) postcontrast T1-weighted images (SE; TR/TE: 500/15 ms) of a 41-year-old patient who developed septic sacroiliitis with abscess formation and joint edema secondary to tonsillitis 60 days earlier. A bizarre abscess cavity is demonstrated with erosive destruction of the joint (*small arrow*) (**A–C**), which is surrounded by contrast-enhancing granulation tissue (*asterisk*) (**A**). Infiltration is seen destroying the capsule and extending into the subperiosteal area of the ilium and into the iliac muscle (*large arrow*) (**C**)

by contrast administration in three of the 11 cases because of early detection of inflammatory alterations. Assessment of the unenhanced images alone including the STIR sequence yielded no clear-cut diagnosis in the three patients with early disease. Both readers rated the diagnostic gain resulting from the contrast-enhanced studies as very high.

Discussion

This study confirms that the plain radiographs were normal in those cases with a short clinical history. The anatomic peculiarities of the normal SIJ and its nonspecific age-related changes [33] make conventional radiographs unreliable in demonstrating early sacroiliitis since the pathologic changes become visible only after several days to weeks [3, 5, 6, 11, 12, 29] and there is a wide intra- and interobserver variation in interpreting sacroiliac radiographs [30]. A study of the SIJs in asymptomatic patients found a high false-positive rate of over 20% [34].

Skeletal scintigraphy using ^{99m}Tc-MDP is a sensitive indicator of inflammatory activity compared with conventional radiographs [5, 6, 8, 35, 36]. Elevated tracer uptake may occur within 2–6 days of the onset of clinical symptoms [3, 5, 15, 19] and is easiest to identify during

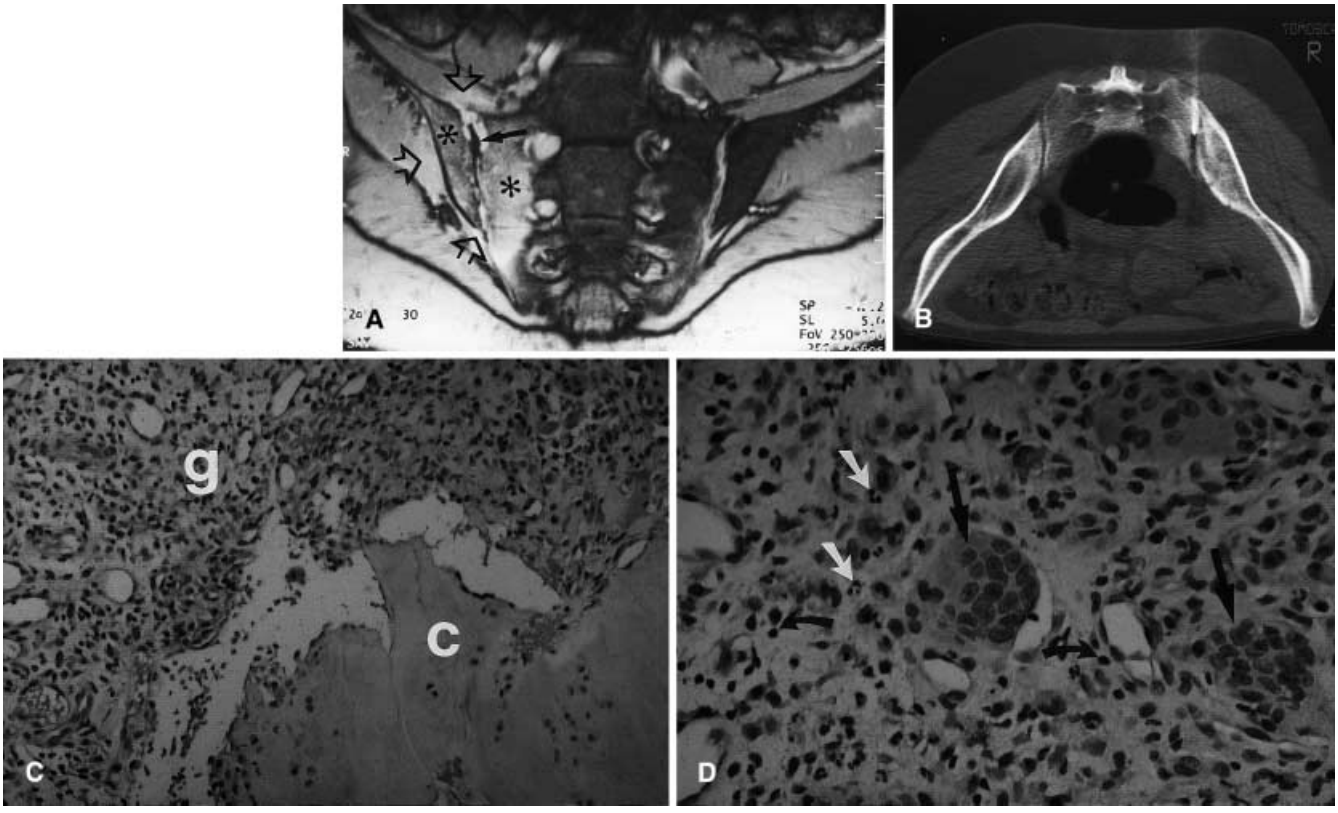

Fig. 4A–C Case 7. T2*-weighted image (**A**) (GE sequence TR/TE: 350/12 ms; flip angle 30° in opposed-phase technique) of a 28-year-old patient obtained 5 weeks after the onset of back pain occurring after delivery. Pseudodilatation of the right joint space is demonstrated, induced by confluent erosions with infiltration of the peri- and para-articular bone marrow (*asterisks*) and transcapsular infiltration of the iliac muscle anteriorly and of the middle gluteal muscle posteriorly (*open arrows*) – the "lava cleft phenomenon". Signal-free intra-articular sequestra without contrast enhancement (*arrow*) are also visible. CT-guided biopsy (**B**) of the right sacroiliac joint using a 2-mm Ostycut bone biopsy needle allowed microbiologic identification of *Streptococcus agalactinae*. H&E-stained histologic sections of the biopsy at ×250 (**C**) and ×500 magnification (**D**) show the interface of granulation tissue (*g*) and hyaline cartilage (*c*). The enlarged detail from **C** shows osteoclastic giant cells (*black arrow*), neutrophilic granulocytes (*oblique white arrow*), and lymphoplasmacytic infiltration (*curved black arrow*) as signs of florid granulating inflammation

the initial phases [10, 29]. However, scintigraphy lacks anatomic detail and cannot differentiate sacroilitiis from a gluteal or psoas abscess and the inflammatory involvement of the periarticular bone [10, 29, 37].

CT of septic sacroiliitis depicts widening of the joint cleft and erosions. Other findings that have been reported are thinning of the periarticular fatty tissue layer, an increase in the size of adjacent muscles, and the occurrence of abscess formation [10, 11]. CT is reported to be almost as sensitive as skeletal scintigraphy and to have the additional advantage of depicting the extent of the inflammatory process [10, 11]. Le Breton et al. [3] report regional muscle swelling to occur within 36 h, which is in agreement with the results of Rafii et al. [38], and suggest that this finding in combination with the presence of destructive osseous changes is indicative of septic sacroiliitis. The authors caution, however, that CT is not suitable for interpreting the early changes associated with septic sacroiliitis such as regional muscle swelling if cortical erosions are absent, enlargement of the joint space is minimal, and inflammatory involvement of adjacent soft tissue occurs without abscess formation [10].

MR imaging provides a high soft tissue contrast even on unenhanced images, resulting in a better differentiation of normal and pathologic tissues compared with CT. Retrospective studies of septic sacroiliitis have shown that MR imaging is more sensitive than CT or skeletal scintigraphy with ^{99m}Tc-MDP [5, 16, 29, 30, 39]. The high soft tissue contrast enables direct assessment of the articular cartilage, of edema of the periarticular bone marrow, and of erosions and fluid within the articular cavity [16, 30]. These rather nonspecific features, which suggest changes in the joint, adjacent soft tissue, and periarticular bone, were reported by several investigators [3, 10, 16, 21, 29].

The common MR features of septic sacroiliitis in our study comprised a reduced SI on T1-weighted images and an elevated SI on T2-weighted/STIR images of the joint space, of the periarticular muscle tissue, and of anterior and/or posterior subperiosteal infiltrations. STIR and T2-weighted images are particularly sensitive for demonstrat-

ing bone marrow edema and inflammatory changes of the adjacent muscle tissue, which have only been seen in patients with septic sacroiliitis [3, 10, 16, 29]. This area of hyperintensity begins in the anterior – seen in our MR imaging study – or posterior joint space, from where it issues subperiosteally along the periarticular bone. We refer to this process as subperiosteal infiltration ("lava cleft phenomenon"). Investigations of the diagnostic assessment of sacroiliitis in SpA by our study group demonstrated pathologic capsular enhancement suggesting inflammation of the capsule, but the inflammatory process never extended to the pericapsular soft tissue [40, 41, 42, 43]. These results underline that the above-described phenomenon is a specific feature of septic sacroiliitis.

The differentiation of septic sacroiliitis from the much more common sacroiliitis in patients with SpA [44] is of utmost clinical relevance since the therapeutic approaches are fundamentally different [40, 41, 42, 43]. The similar MR features are contrast-enhancing intra-articular spaces and erosions, anterior or posterior enhancement of the capsule, and bone marrow edema. The triad of symptoms typical for late sacroiliitis in SpA, consisting of erosion, subchondral sclerosis, and formation of transarticular bone bridges, was found neither in any of our 11 patients with septic sacroiliitis nor in any patients reported in the literature [10, 16, 30]. The above-described "lava cleft phenomenon" is absent in the reported cases of sacroiliitis in SpA (personal data: more than 1000 cases investigated). Another feature of septic sacroiliitis, the infiltration of pericapscular layers of the iliopsoas and gluteal muscles, is likewise not seen in the reported forms of sacroiliitis in SpA [40, 41, 42, 43].

Advanced stages of septic sacroiliitis were always characterized by the demonstration of erosion, sequestration, and abscess formation [10, 16]. The latter two are complications of septic sacroiliitis occurring when antibiotic treatment is delayed or inappropriate [7]. Sequestration and abscess formation do not occur in SpA sacroiliitis [42], whereas erosions are seen as contrast-enhancing areas, often associated with pseudodilatation of the joint, in both septic and SpA sacroiliitis [43].

Sandrasegaran et al. [10] regard the combination of clinical symptoms, the blood culture findings, and the changes seen at MR imaging as sufficient for establishing the diagnosis of septic sacroiliitis and initiating antibiotic therapy. We think that the demonstration of septic sacroiliitis by MR imaging should always be followed by the targeted microbiologic confirmation of the pathogen, including the determination of its resistance. The most reliable method to obtain material seems to be CT-guided puncture of the SIJ [5, 11] whenever blood culture fails to isolate the pathogen [18, 25].

MR imaging is the only imaging modality to reliably assess progression or regression at follow-up and to thus draw the proper therapeutic conclusions. A discrepancy was notable in our patients between a rather early clinical improvement after initiation of antibiotics and a much later regression of changes seen on MR images. This early clinical improvement might mimic resolution, and there is a risk of discontinuing therapy too soon.

Erdmann et al. [45] described changes in periarticular bone marrow caused by septic arthritis (among them two cases of septic sacroiliitis) as pitfalls in the diagnosis of osteomyelitis. Rosenberg et al. [6] reported a case of septic sacroiliitis associated with secondary osteomyelitis. Haliloglu et al. [29] examined five cases of acute septic sacroiliitis or sacroiliac osteomyelitis by MR imaging and skeletal scintigraphy and concluded that a definitive differentiation of osteomyelitis and sacroiliitis was not possible. While MR imaging is reported to depict inflammatory bone changes with a sensitivity similar to that of scintigraphy, its specificity of over 90% resulting from the better spatial resolution and the high soft tissue contrast is superior to the specificity of only 65% of scintigraphy [46, 47]. Today the sensitivity of MR imaging for depicting septic musculoskeletal processes can be improved by means of fat-suppressed contrast-enhanced studies and STIR sequences [48]. It is possible that a large number of the cases of osteomyelitis of the sacrum and/or ilium presented in the literature are late sequelae of inadequately treated septic sacroiliitis.

Despite the low number of patients, the current study has identified clear-cut morphologic MR imaging features of septic sacroiliitis that are different from reported findings of sacroiliitis in SpA. The findings by MR imaging make it possible to initiate specific treatment before destruction of the joint occurs. The low number of patients with septic sacroiliitis, especially of patients with early disease, limits the impact of our results. Given the rarity of the disease, multicenter trials are therefore needed to definitively establish the crucial role which we believe MR imaging has in reliably diagnosing septic sacroiliitis.

References

1. Bellamy N, Park W, Rooney PJ. What do we know about the sacroiliac joint? Semin Arthritis Rheum 1983; 12:282–313.
2. Coy JT, Wolf CR, Brower TD, Winter WG. Pyogenic arthritis of the sacroiliac joint. J Bone Joint Surg Am 1976; 58:845–849.
3. Le Breton C, Frey I, Carette MF, et al. Infectious sacroiliitis: value of computed tomography and magnetic resonance imaging. Eur Radiol 1992; 2:233–239.
4. Moyer RA, Bross JE, Harrington TM. Pyogenic sacroiliitis in a rural population. J Rheumatol 1990; 17:1364–1368.

5. Zimmermann B, Mikolich DJ, Lally EV. Septic sacroiliitis. Semin Arthritis Rheum 1996; 26:592–604.
6. Rosenberg D, Baskies AM, Deckers PJ, Leiter BE, Ordia JI, Yablon IG. Pyogenic sacroiliitis: an absolute indication for computerized tomographic scanning. Clin Orthop 1984; 184:128–132.
7. Schaad UB, McCracken GH, Nelson JD. Pyogenic arthritis of the SIJ in pediatric patients. Pediatrics 1980; 66:375–379.
8. Gordon G, Kabins SA. Pyogenic sacroiliitis. Am J Med 1980; 69:50–56.
9. Abbott JT, Carty H. Pyogenic sacroiliitis, the missed diagnosis? Br J Radiol 1993; 66:120–122.
10. Sandrasegaran K, Saifuddin A, Coral A, Wutt WP. Magnetic resonance imaging of septic sacroiliitis. Skeletal Radiol 1994; 23:289–292.
11. Bankoff MS, Sarno RC, Carter BL. CT scanning in septic sacroiliac arthritis or periarticular osteomyelitis. Comput Radiol 1984; 8:165–170.
12. Carlson SA, Jones JS. Pyogenic sacroiliitis. Am J Emerg Med 1994; 12:639–641.
13. Wilbur AC, Langer BG, Spigos DG. Diagnosis of sacroiliac joint infection in pregnancy by MR imaging. Magn Reson Imaging 1988; 6:341–343.
14. Brancos MA, Peris P, Miro JM, et al. Septic arthritis in heroin addicts. Semin Arthritis Rheum 1991; 21:81–87.
15. Guyot DR, Manoli A, Kling GA. Pyogenic sacroiliitis in IV drug abusers. AJR 1987; 149:1209–1211.
16. Klein MA, Winalski CS, Wax MR, Piwnica-Worms DR. MR imaging of septic sacroiliitis. J Comput Assist Tomogr 1991; 15:126–132.
17. Bowen V, Cassidy JD. Macroscopic and microscopic anatomy of the sacroiliac joint from embryonic life until the eighth decade. Spine 1981; 246:146–149.
18. Vyskocil JJ, McIlroy MA, Brennan TA, Wilson FM. Pyogenic infection of the sacroiliac joint: case reports and review of the literature. Medicine 1991; 70:188–197.
19. Feldmann JL, Menkes CJ, Weill B, Delrieu F, Delbarre F. Les sacro-iliites infectieuses: étude multicentrique sur 214 observations. Rev Rhum 1981; 48:83–91.
20. Hodgson BF. Pyogenic sacroiliac joint infection. Clin Orthop 1989; 246:146–149.
21. Mitchell M, Howard B, Haller J, Sartoris DJ, Resnick D. Septic arthritis. Radiol Clin North Am 1988; 26:1295–1313.
22. Goldberg J, Kovarsky J. Tuberculous sacroiliitis. South Med J 1983; 76:1175–1176.
23. Pouchot J, Vinceneux P, Barge J, et al. Tuberculosis of the sacroiliac joint: clinical features, outcome, and evaluation of closed needle biopsy in 11 consecutive cases. Am J Med 1988; 84:622–628.
24. Ariza J, Pujol M, Valverde J, et al. Brucellar sacroiliitis: findings in 63 episodes and current relevance. Clin Infect Dis 1993; 16:761–765.
25. Bronze MS, Whitby S, Schaberg DR. Group G streptococcal arthritis: case report and review of the literature. Am J Med Sci 1997; 313:239–243.
26. Dunn EJ, Bryan DM, Nugent JT, Robinson RA. Pyogenic infection of the sacroiliac joint. Clin Orthop 1976; 118:113–117.
27. Avila L. Primary pyogenic infection of the sacroiliac articulation: a new approach to the joint. J Bone Joint Surg 1941; 23:922–928.
28. Cohn SM, Schoetz DJ. Pyogenic sacroiliitis: another imitator of the acute abdomen. Surgery 1986; 100:95–98.
29. Haliloglu M, Kleinmann MB, Siddiqui AR, Cohen MD. Osteomyelitis and pyogenic infection of the sacroiliac joint. Pediatr Radiol 1994; 24:333–335.
30. Murphey MD, Wetzel LH, Bramble JM, Levine E, Simpson KM, Lindsley HB. Sacroiliitis: MR imaging findings. Radiology 1991; 180:239–244.
31. Reilly JP, Gross RH, Emans JB, Yngve DA. Disorders of the SIJ in children. J Bone Joint Surg Am 1988; 70:31–40.
32. Braun J, Bollow M, Sieper J. Radiologic diagnosis and pathology of the spondylarthropathies. Rheum Dis Clin North Am 1998; 24:697–735.
33. Forrester D. Imaging of the SIJ. Radiol Clin North Am 1990; 28:1055–1072.
34. Cohen AS, McNeill JM, Callius E, Sharp, JT, Schubart A. The “normal” sacroiliac joint: analysis of 88 sacroiliac roentgenograms. AJR 1967; 10:559–563.
35. Delbarre F, Rondier J, Delrieu F, et al. Pyogenic infection of the sacroiliac joint. J Bone Joint Surg Am 1975; 17:819–825.
36. Trauner DA, Connor JD. Radioactive scanning in diagnosis of acute sacroiliac osteomyelitis. J Pediatr 1975; 87:751–753.
37. Siddiqui AR. Nuclear imaging in paediatrics. Chicago: Year Book, 1985:229–272.
38. Rafii M, Firooznia H, Golimbu C. Computed tomography of septic joints.CT 1985; 9:51–60.
39. Morrison WB, Schweitzer ME, Bock GW, et al. Diagnosis of osteomyelitis: utility of fat-suppressed contrast-enhanced MR imaging. Radiology 1993; 189:251–257.
40. Bollow M, Braun J, Biedermann T, et al. Use of contrast-enhanced MR imaging to detect sacroiliitis in children. Skeletal Radiol 1998; 27:606–616.
41. Bollow M, Braun J, Hamm B, et al. Early sacroiliitis in patients with spondylarthropathy: evaluation with dynamic gadolinium-enhanced MR imaging. Radiology 1995; 194:529–536.
42. Bollow M, Braun J. Sakroilikalgelenk. In: Reiser M, Vahlensieck M, eds. MR imaging of the musculoskeletal system. Stuttgart: Thieme, 1997:359–379.
43. Bollow M, Loreck D, Braun J, Hamm B. Sacroiliitis: the key symptom in spondylarthropathies. 2. Morphological aspects. Fortschr Rontgenstr 1997; 166:275–289.
44. Braun J, Bollow M, Remlinger G, et al. Prevalence of spondylarthropathies in HLA-B27 positive and negative blood donors. Arthritis Rheum 1998; 41:58–67.
45. Erdmann WA, Tamburro F, Jayson HT, Weaterall PT, Ferry KB, Peshock RM. Osteomyelitis: characteristics and pitfalls of diagnosis with MR imaging. Radiology 1991; 180:533–539.
46. Unger E, Modofsky P, Gatenby R, Hartz W, Broder G. Diagnosis of osteomyelitis by MR imaging. AJR 1988; 150:605–610.
47. Zynamon A, Jung T, Hodler J, Bischof T, Schulthess GK. Magnetic resonance for the diagnosis of osteomyelitits. Fortschr Rontgenstr 1991; 155:513–518.
48. Vahlensieck M, Seelos K, Träber F, Gieseke J, Reiser M. MR tomography with fast STIR technique: optimization and comparison with other sequences in a 0.5 tesla system. Fortschr Rontgenstr 1993; 159:288–294.